




Open Archive Toulouse Archive Ouverte (OATAO)

OATAO is an open access repository that collects the work of Toulouse researchers and makes it freely available over the web where possible

This is an author's version published in: <http://oatao.univ-toulouse.fr/25161>

Official URL: <https://doi.org/10.1016/j.cep.2017.07.025>

To cite this version:

You, Xinqiang and Gu, Jinglian and Peng, Changjun and Rodríguez-Donis, Ivonne  and Liu, Honglai *Optimal design of extractive distillation for acetic acid dehydration with N-methyl acetamide*. (2017) *Chemical Engineering and Processing: Process Intensification*, 120. 301-316. ISSN 0255-2701

Any correspondence concerning this service should be sent to the repository administrator: tech-oatao@listes-diff.inp-toulouse.fr

Optimal design of extractive distillation for acetic acid dehydration with N-methyl acetamide

Xinqiang You^a, Jinglian Gu^b, Changjun Peng^a, Ivonne Rodriguez-Donis^{c,*}, Honglai Liu^a

^a State Key laboratory of Chemical Engineering and Department of Chemistry, East China University of Science and Technology, Shanghai 200237, China

^b School of Chemistry and Chemical Engineering, Chongqing University, Chongqing 400044, China

^c Laboratoire de Chimie Agro-Industrielle, Université de Toulouse, INRA, ENSIACET-INPT, Toulouse, France

ARTICLE INFO

Keywords:

Acetic acid dehydration
Extractive distillation
Sequential quadratic programming
Multi-objective optimization
Genetic algorithm

ABSTRACT

A distinctive strategy for entrainer recycling is proposed in this work for acetic acid (AA) dehydration by extractive distillation by using N methyl acetamide (NMA). The use of standard entrainers such as DMF or DMSO has the main drawback of forming an azeotrope with acetic acid. However, the vapour liquid equilibrium AA – NMA exhibits a tangential pinch point at NMA end composition. The new strategy rises from the thermodynamic analysis of the ternary diagram that which involves no azeotrope. As a result, acetic acid with high purity can be obtained by the recycling of the entrainer with a relaxed constraint in its purity. Optimization studies are discussed by using two approaches: two-step optimization method with Sequential Quadratic Programming (TSOM case) and the multi-objective genetic algorithm. The multi-objective genetic algorithm allowed the computation of the optimal acetic acid dehydration with an impurity of 3% in the recycled entrainer. Significant cost savings are achieved thanks to the optimization of both columns together. Energy consumption is reduced by 12.8% and 56.9% whereas TAC is saved by 28.4% and 56.3% compared with optimal case TSOM (impurity content 1%) and a published “Case Ref” (impurity content 0.01%), respectively.

1. Introduction

Acetic acid (AA), as an important solvent or reagent, is widely used in many fine chemical or petrochemical processes. Aqueous solution of AA is produced as by products in wood distillate (1.8 wt% AA) [1], manufacturing of cellulose acetate from acetylation of cellulose (35 wt%) [2], and synthesis of terephthalic acid process (about 65 wt%) [3]. Therefore, the dehydration of aqueous AA in an economical way is of great importance for the industries above and others, such as methyl acetate production, ketene production and various methods for the concentration of AA [4,5]. However, it is difficult to separate AA from water by simple distillation because the relative volatility between water and AA is close to unit (see Fig. 1) mainly in the region of increasing water purity. Therefore, advanced processes such as pressure swing distillation, azeotropic distillation, reactive distillation and extractive distillation are required. First, the pressure swing distillation is overlooked since the vapor liquid equilibrium of AA and water is not sensitive enough to the pressure. Second, according to the study of Furum and Fonyo [4], azeotropic distillation could be only used for separating AA solution with AA content greater than 35 wt%. Later, Wasylkiewicz et al. [6] proposed a geometric method for the design of

AA dehydration azeotropic distillation based on the examination of the whole composition space. Chien et al. [7] studied the separation of equimolar mixture of AA water via heterogeneous azeotropic distillation, and iso butyl acetate was found the best azeotropic entrainer. For more dilute feeds, AA enrichment is necessary. One way for AA enrichment is solvent extraction, and the solvent could be ethyl acetate, isopropyl acetate, diethyl ether and so on [3]. However, the solvent extraction is limited by phase separation and the distribution of impurities. Besides, the high amount of solvents would cause much energy consumption for solvent recovery by vaporization. Another way is to use a pre concentrator column for the enrichment of AA. Chien and Kuo [8] studied the necessity of adding pre concentrator column before azeotropic distillation column for the dehydration of dilute AA, and they found the surprise that no pre concentrator flowsheet was better than the pre concentrator flowsheet following the total annual cost (TAC). Third, the reactive distillation for recovery of dilute AA is described by Saha et al. [2] by using n butanol/iso amyl alcohol as esterification solvent and by Lei et al. [9] by employing tributylamine as separating agent. Although a value added ester is formed, an additional column is needed for the whole process.

Extractive distillation, as an alternative process, that usually

* Corresponding author.

E-mail address: ivonne.rodriguezdonis@ensiacet.fr (I. Rodriguez-Donis).

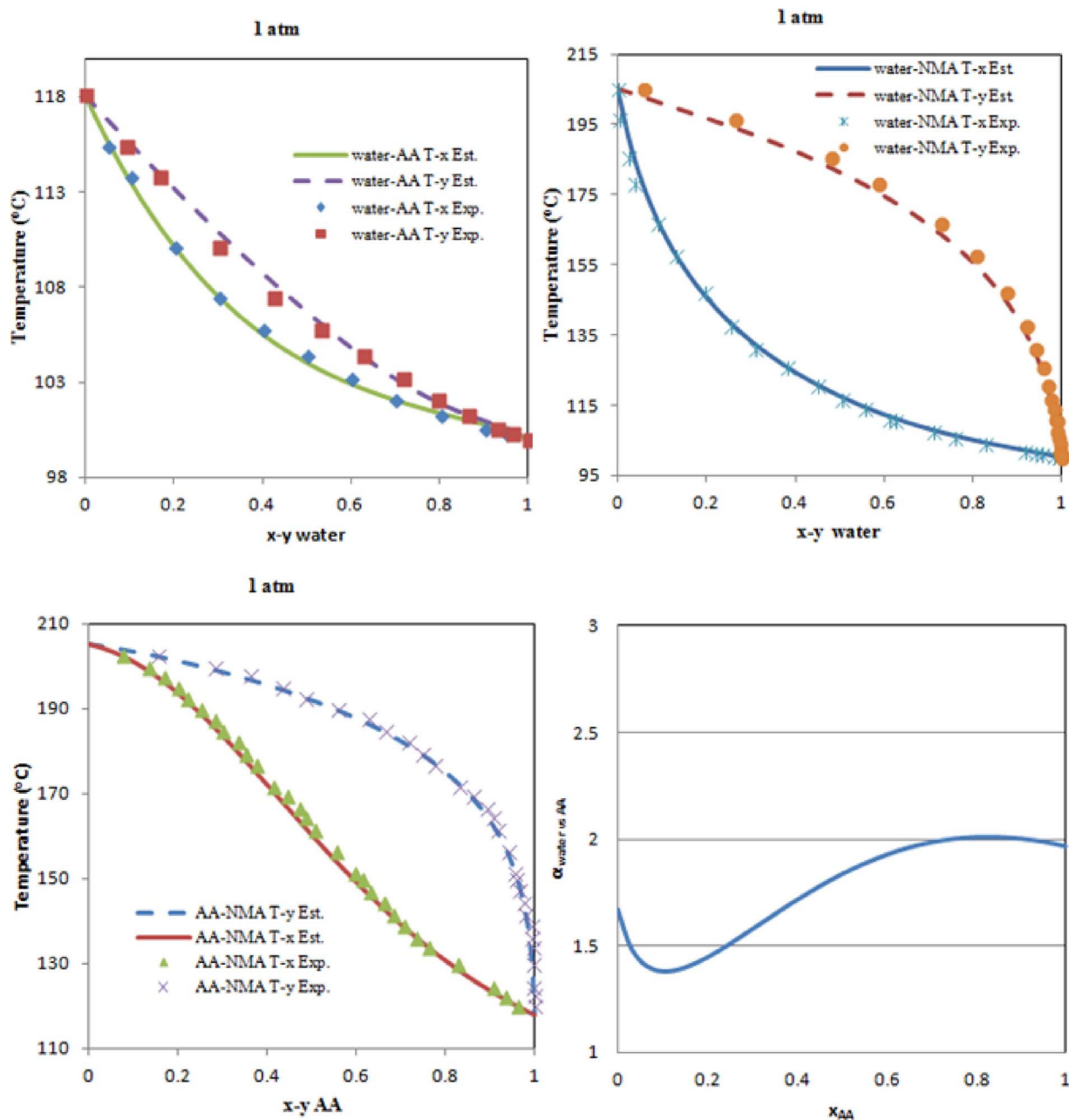


Fig. 1. Volatility and T-xy experiment and predicted map of water-AA-NMA system at 1 atm.

requires a relative low energy consumption because of low reflux ratio and provides simplification in design and control. For the dehydration of AA by extractive distillation, there are plenty of publications focusing on the selection of entrainers, such as 1,2 dimorpholinoethane [10], *N* methyl acetamide (NMA) [11], *N* methyl 2 pyrrolidone (NMP) [12], sulfolane, adiponitrile, dimethylsulfoxide [13] and so on. Hu and Zhou [14] verified that NMA and NMP are the better entrainers for the dehydration of AA solution based on the experimental data as the two candidates have much better performances on increasing the relative volatility of water as we will discuss in the next section. However, to the best of our knowledge, very few publications have investigated the design and optimization of extractive distillation for the dehydration of AA. The main reason is probably that there is a tangential behavior of the binary VLE between the AA and entrainer and it will be difficult to save energy and capital cost compared with the conventional distillation process. Hence, some strategic modifications have to be done for the optimal design of AA dehydration process in order to enhance the

benefits of the extractive distillation process.

In this work, the optimal design of the extractive distillation process for AA dehydration by using NMA as entrainer is completely investigated. A new counter intuitive strategy is developed: high contents of impurities in the recycled entrainer for the extractive distillation is firstly proposed based on the knowledge of thermodynamic features of the residue curve map (RCM) of the ternary mixture water-AA-NMA. The topological structure of RCM corresponds to Serafimov's class 0.0 1 [15] with no existence of univolatility lines between any pairs of components. The steady state process is optimized through keeping a high purity of AA in the distillate of the regeneration column while the recycled entrainer in the bottom liquid is specified with high contents of impurities. This strategy is completely differing from the ideology of the Serafimov's class 1.0 1a, in which the low content of impurities in the recycled entrainer is compulsory, otherwise, the high purity of the distillate of the extractive distillation column would not be obtained no matter how large is the reflux ratio. Here the low contents of impurities

in the recycled entrainer ($x_{L,I,E}$) means that its value is lower than 1×10^{-4} and this is a normal specification for ternary diagram class 1.0 1a while the high contents of impurities in the recycled entrainer ($x_{H,I,E}$) represents that its value is higher than 20×10^{-4} . The essential differences are that the distillate product of the extractive column for ternary diagram class 0.0 1 is an extractive stable node while it is an extractive saddle for class 1.0 1a. The proposed strategy enables to save energy cost by alleviating the tangential behavior of VLE between AA and NMA at high composition of the entrainer. In order to illustrate the benefits of the new strategy, two optimization methods are used: (1) two step optimization approach (TSOM) by using SQP method and (2) multi objective genetic algorithm (MOGA).

The reminder of this work is organized as following. Section 2 presents the thermodynamic insights of the RCM of the ternary diagram belonging to Serafimov's class 0.0 1 as well as the description of both optimization methods. The results and discussions are shown in Section 3. It firstly supplies the thermodynamic analysis of AA dehydration process and the choice of the distillate flow rates obeying their inter relationships. The results of TSOM are also discussed to illustrate the benefits of the new strategy under specified $x_{H,I,E}$ at a fixed total tray number of both columns. Thirdly, MOGA is employed to optimize the $x_{H,I,E}$ and the tray numbers of columns and the optimization results are explained by analyzing the liquid profile into the extractive column into the map of the isovolatility curves of the ternary mixture. Conclusions points out the major impact and significance of our findings.

2. Background, methods and objective functions

2.1. Thermodynamic insights of the extractive distillation process

The simulation of AA dehydration with the entrainer NMA was carried out by using simulator Aspen plus V7.3. The NRTL HOC property method that uses the Hayden O'Connell equation of state as the vapor phase model and NRTL [16] for the liquid phase was used for the prediction of the vapor liquid equilibrium (VLE) in these simulations. AA molecules strongly associate with each other due to the hydrogen bond between two molecules. Hence, the association effect on vapour liquid equilibrium cannot be neglected even at low pressure. The Hayden O'Connell equation reliably predicts the solvation of polar compounds and dimerization in the vapor phase that occurs with mixtures containing carboxylic acids [17]. The association parameters shown in Table A1 in Appendix B were adopted to calculate the fugacity coefficients. Computation of ternary vapour liquid equilibrium was performed by using NRTL HOC property method available in Aspen plus V7.3 software along with the binary coefficients for AA water and NMA water. Binary parameters for AA NMA were taken from Chang et al. [18] based on the experimental data. All binary parameters are shown in Table B1 in Appendix B. The saturated vapor pressure of the pure components was calculated by the extended Antoine equation. The accuracy of the models and parameters was verified for each binary mixture by comparing the computed with experimental values from Dechema [19] as it is shown in Fig. 1.

Fig. 1 shows the good agreement between the estimated values with the experimental data. It demonstrates that the selected thermodynamic model and the binary parameters are able to well describe the ternary system of water AA NMA. We also notice that there is a tangent point between AA and NMA at NMA rich composition part. It leads to an unusual design of extractive distillation process by using NMA as entrainer for separating water AA after NMA is reported as a suitable entrainer with high relative volatility and selectivity [12].

Fig. 2 displays the RCM and the map of isovolatility curves for the main entrainers applied, DMF and DMSO [13] and NMA and NMP [12], for separating the binary mixture water AA by extractive distillation process. Isovolatility curves were computed using Simulis Thermodynamics[®] property server package and services available in Excel [20]. Binary coefficients for binary mixtures of water and the entrainers DMF,

DMSO and NMP were taken from the database available in Aspen plus V7.3 whereas those involving AA were taken from Chang et al. [18] and Peng et al. [21].

Following remarks can be done from the analysis of thermodynamic properties of the ternary diagrams in Fig. 2:

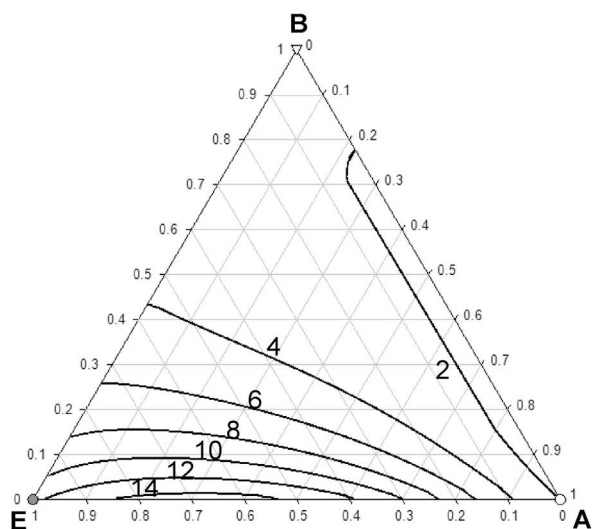
- All ternary diagrams belong to Serafimov's class 0.0 1 and the univolatility curve between water AA doesn't exist for all entrainers. Water is the most volatile component in the entire composition space providing the distillate product of the extractive distillation column. Hence, the binary mixture of AA and the entrainer will be the bottom product and its separation takes place in a second distillation column (entrainer recovery column) where the acetic acid is the distillate product. Classic entrainers for extractive distillation processes as DMF and DMSO have the key drawback of forming a binary maximum azeotropic mixture (BE) with acetic acid. RCM belongs to ternary diagram of Serafimov's class 1.0 1a. RCM doesn't exhibit any distillation boundaries and water remains as the most volatile component. However, the bottom product from the entrainer recovery column will be the binary maximum azeotrope AA – E having a negative impact over the recovery yield of AA.
- DMF exhibits the highest values of isovolatility when the entrainer composition is increased in the resulting ternary mixture. However, DMSO with a greater boiling temperature allows decreasing the AA composition in the maximum boiling binary azeotrope and hence, theoretically increasing the recovery yield of AA. Using entrainers as NMA and NMP provided both advantages, not formation of any binary azeotrope in the resulting ternary mixture and high values of relative volatility water AA with the increasing of entrainer composition. Therefore, separation of water from acetic acid can be performed under more favorable operating conditions such as lower entrainer flowrate and reflux ratio.

The variation of the RCM and the map of the extractive liquid profiles for the ternary diagram class 0.0 1 is displayed in Fig. 3 when the separation of the components A and B is carried out by a batch extractive distillation column under a feeding of the entrainer in an upper tray of those of the main binary feeding A B and at finite reflux ratio as it was highlighted out by Rodriguez Donis et al. [22].

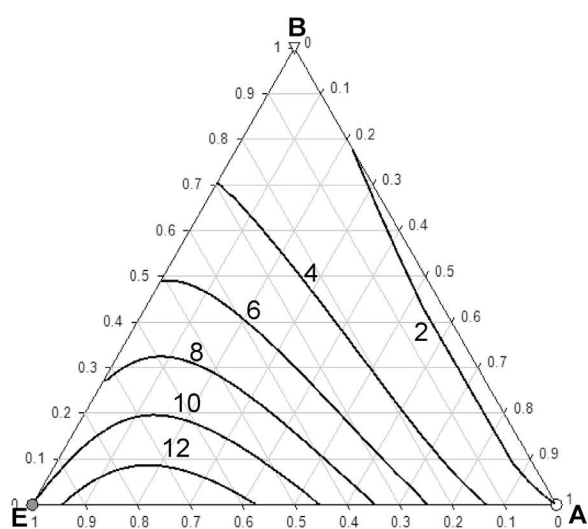
Component A is the sole residue curve unstable node (see Fig. 3a) and will be the column top product under infinite reflux operation and no entrainer feeding. This is why a conventional distillation without using an external entrainer but implicating a very high reflux ratio is a feasible process for the separation of water AA mixture. As explained through bifurcation theory [23], the extractive liquid profile map singular points are identical to residue curve map (RCM) points but with opposite stability. Therefore, the vertex A in Fig. 3b is the unstable node UN_{rcm} in the RCM but the stable extractive node $SN_{ext,A}$. Vertex B is the saddle node S_{rcm} in the RCM and the extractive singular point $S_{B,ext}$. Vertex E is stable node SN_{rcm} in the RCM but the unstable extractive node UN_{ext} . Note that the edges E A, B E, and A B are unstable, unstable, and stable extractive separatrices at infinite reflux, respectively.

At infinite reflux, as soon as the entrainer feed ratio is turned on ($F_E/V > 0$), an extractive column section arises, between the entrainer feed tray and the azeotropic main feed tray, which links the liquid profiles of the rectifying section with those of the stripping section. Both, the extractive stable node $SN_{ext,A}$ and saddle $S_{B,ext}$ then move toward vertex E over the binary side E A and B E respectively (see Fig. 3c). Linking $SN_{ext,A}$ and $S_{B,ext}$, the stable extractive separatrix moves from the A B edge inside the ternary diagram. Enough trays should be used in the extractive section to make all the extractive profiles reach $SN_{ext,A}$ in order to intersect a residue curve ending at vertex A following the decreasing direction of temperature. Consequently, component A is settled at the top of the column. There is no minimum value for F_E/V because the univolatility line α_{AB} does not

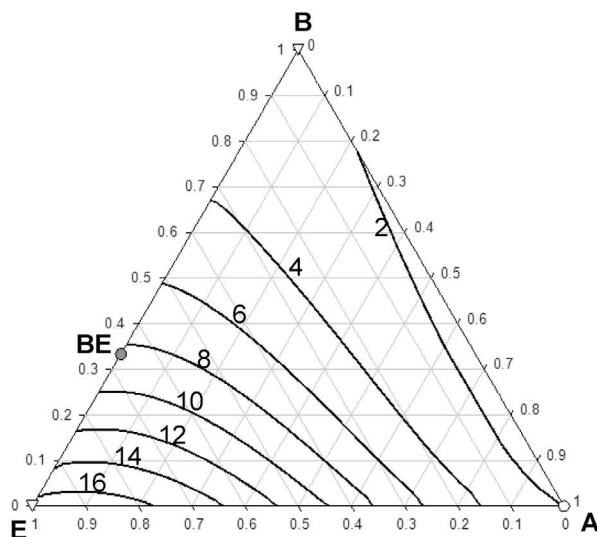
(a) Entrainer: NMA(BP = 204-206°C)



(b) Entrainer: NMP(BP = 202-204°C)



(c) Entrainer: DMF(BP = 153°C)



(d) Entrainer: DMSO(BP = 189°C)

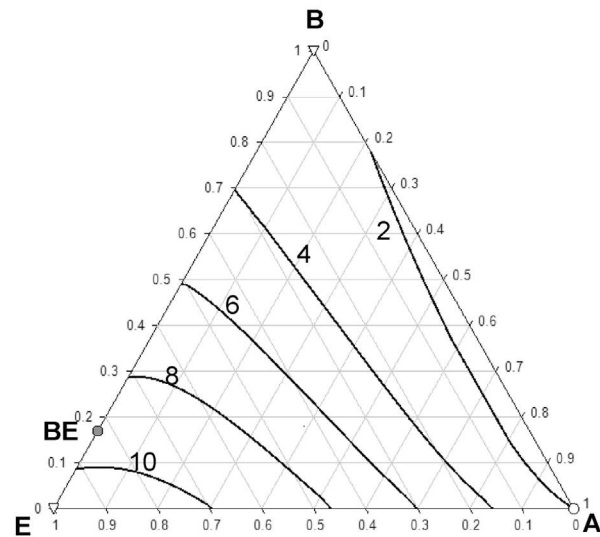


Fig. 2. Map of Isovolatility curves of the ternary mixtures water (A) – AA(B) – entrainers(E).

exist.

Distillate withdrawal requires the operation under a finite reflux keeping the entrainer feeding (Fig. 3d). Hence, the location of singular points and separatrices change. The saddle point $S_{B,ext}$ leaves the binary side B E and moves inside the ternary diagram. It drags along the unstable extractive separatrix $UN_{ext} S_{ext} UN_{ext}'$, above which lies the unfeasible region as the corresponding extractive profiles cross the B E edge toward an outside stable extractive node $SN_{ext,B}'$ and no intersection with the residue curve going to A occurs. From a composition in the feasible region, the still composition path moves according to the vector cone shown in Fig. 3d and may cross the unstable extractive separatrix, preventing the total recovery of component A from the column. The F_E/V in batch mode could be transferred into F_E/F in continuous mode by the equation in literature [24].

2.2. Design flowsheet and process optimization techniques

2.2.1. Modification of the process flowsheet

The design flowsheet of extractive distillation for separating low relative volatility mixture is shown in Fig. 4 as it is set in Aspen Plus. The main feed (water – AA) is entered into the extractive column at one stage whereas the entrainer NMA is fed at another upper stage, so there is an extractive section between both feedings allowing the increasing of the relative volatility of water, thus enabling the separation of the key components. Water is separated as distillate product D_1 while the bottom product is the mixture AA and NMA (F_2) that is fed to the second column. High purity AA is separated as distillate D_2 in the second column. Most importantly, by following the proposed strategy, the impurity composition of stream W_2 will be $x_{H,I,E}$ instead of $x_{L,I,E}$. Subsequently, how to deal with the variable of $x_{H,I,E}$ in W_2 ? First, in the TSOM method, it is specified in advance in the open loop flow sheet in

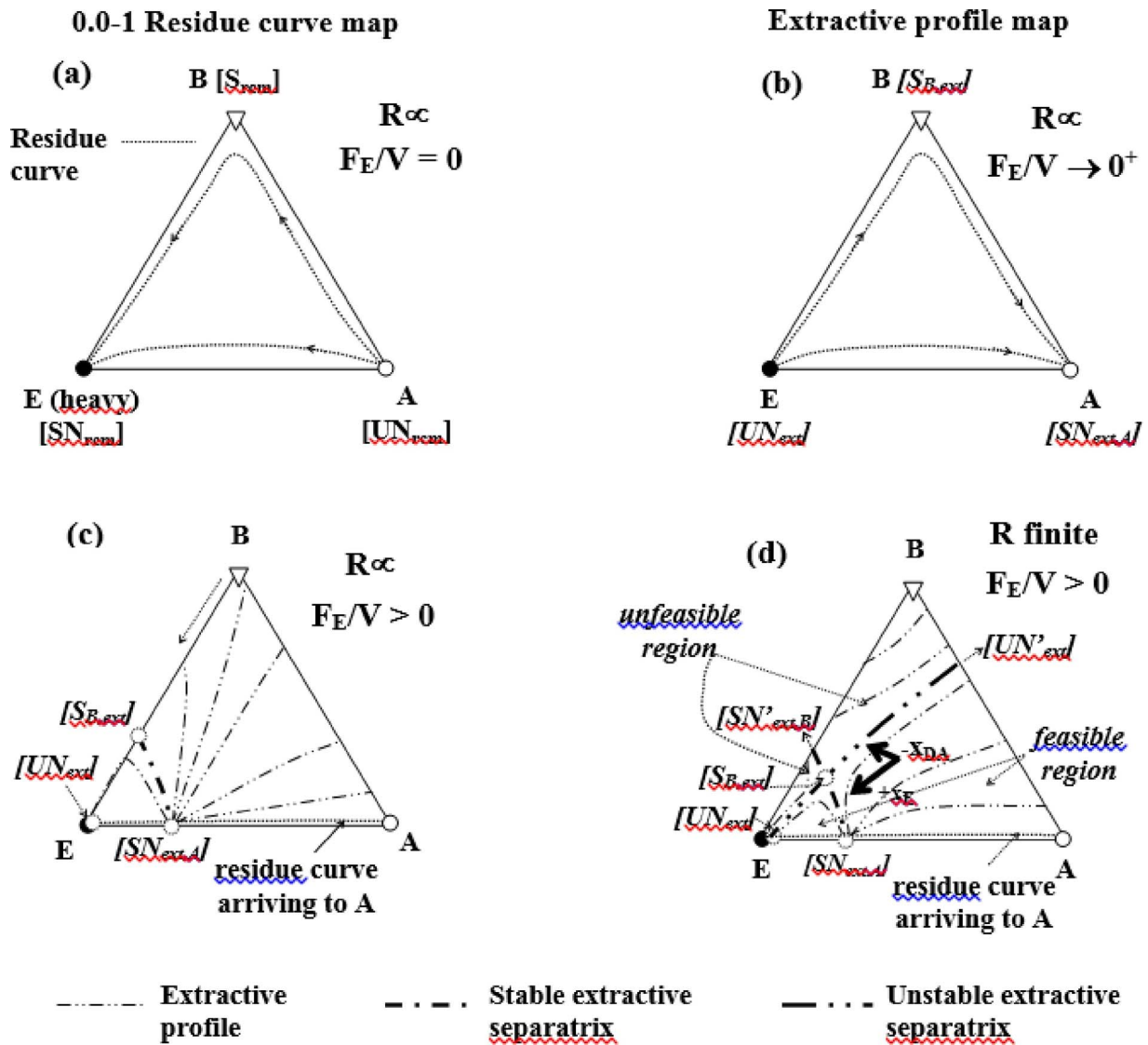


Fig. 3. Influence of the reflux ratio and entrainer feed flow rate on extractive singular points of class 0.0-1 diagram in batch mode operation. (Adapted from Rodriguez-Donis et al. [22])

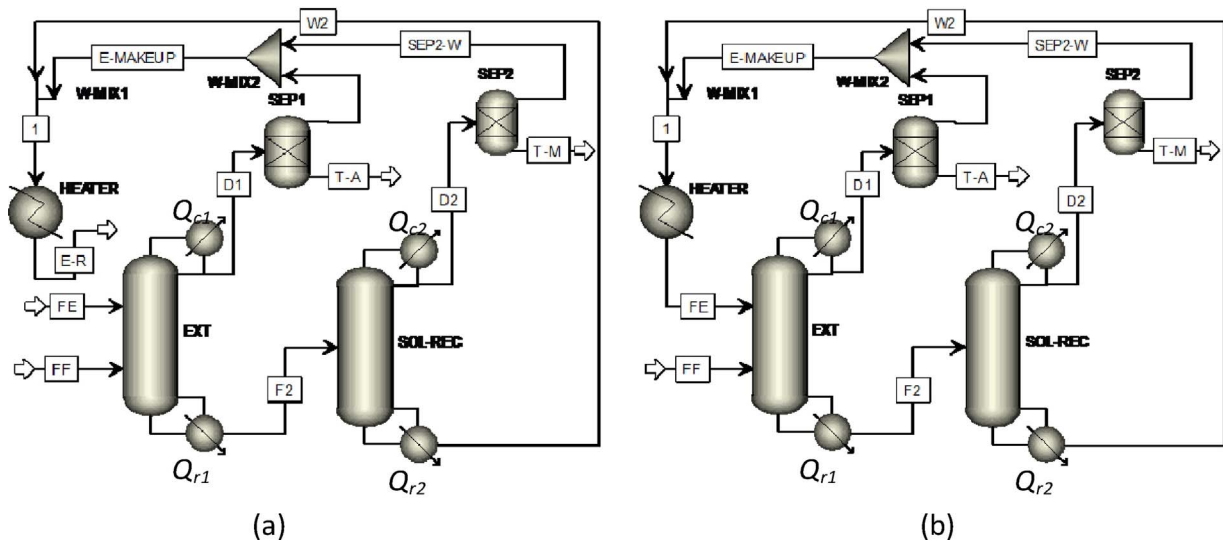


Fig. 4. Design flow sheet of extractive distillation process, (a) open loop, (b) close loop.

Fig. 4a, and after optimization the results are systematically checked within the close loop flow sheet that corresponds to the industrial plant, where the entrainer is practically recycled (Fig. 4b). Further in the MOGA method, the impurity composition in the recycled entrainer $x_{H,I,E}$ is treated as another optimization variable directly in the close loop flowsheet in Fig. 4b. The process flowsheet needs a make up entrainer (NMA) to compensate its losses in the two distillates. As the NMA losses is not known beforehand, we obtain it through introducing sharp splits (sep1 and sep2) on the two distillate products. Finally, the pressure drop per stage is regarded as 0.0068 atm in each column that operates at constant top pressure.

It is worth mentioned that the closed loop flowsheet can deal with the both situations, the low contents of impurities in the recycled entrainer (strategy $x_{L,I,E}$) and the high contents of impurities in the recycled entrainer (strategy $x_{H,I,E}$).

2.2.2. Two step optimization methodology (TSOM)

For an extractive distillation process retrofit (given column trays number N_1 and N_2), the two step optimization methodology has shown many advantages for optimization studies of others extractive distillation processes [24–26]. First, considering open loop flow sheet with no entrainer recycled, fresh pure entrainer is fed into the extractive column to ease the convergence of the process, and the sequential quadratic programming (SQP) method is used for process optimisation under product purity and recovery constraints. The manipulating variables are column reflux ratios R_1 , R_2 and the entrainer flow rate F_E . Secondly, a sensitivity analysis is performed to find the optimal values of two distillate flow rates and the three feed tray locations N_{FE} , N_{FAB} , N_{FReg} , while SQP is run for each set of discrete variable values. An available design in literature [25] here called “Case Ref” is employed as initial values of the optimization study using TSOM approach. The final optimisation is found through minimizing OF value and it is validated by rerunning the simulation in close loop flow sheet where the entrainer is recycled from the regeneration column to the extractive column and also adding an entrainer make up feed. Notice that the close loop simulation requires adjusting the reflux ratio if necessary in order to overcome the effect of impurities in recycled entrainer on both distillate purity. Finally, the TAC is calculated to compare the different designs.

2.2.3. Multi objective genetic algorithm

Using stochastic methods such as genetic algorithms together with simultaneous process simulators in commercial software has become attractive for a total new extractive distillation process design in solving optimization problems due to the following characteristics. First, the convergence of the process simulator relies upon reasonability of the initial input value. The simulator may fail to converge when unsuitable initial input values are set. This issue is less important in the stochastic optimization technique because the search for optimal solution in genetic algorithm is not limited to one point but rather based on several points simultaneously which build the population [26]. Second, it is unnecessary to display the precise information of the mathematical model or its derivatives because the algorithms are based on a direct search method.

Inspired by the study of Vazquez Ojeda et al. [27] the multi objective genetic algorithm in Matlab was directly linked with simulator in Aspen plus. Aspen plus tools named *variable explorer* was used for finding the node of variables like reflux ratio, distillate and tray number in column. The MESH model *Radfrac* in Aspen Plus was adopted for the process simulation. In this way, genetic algorithm works for optimization meanwhile Aspen plus was employed for process simulation and handling $x_{H,I,E}$ with Wegstein tear method.

Inspired by the study of Vazquez Ojeda et al. [27] the multi objective genetic algorithm in Matlab was directly linked with simulator in Aspen plus. *Variable explorer* tool available in Aspen plus was used for finding the node of variables like reflux ratio, distillate and tray number in column. The MESH model *Radfrac* in Aspen Plus was adopted for the

process simulation. In this way, genetic algorithm works for optimization meanwhile Aspen plus was employed for process simulation and handling $x_{H,I,E}$ with Wegstein tear method. This was proved as a suitable way to directly optimize the closed loop configuration with all discrete and continuous variables under the multi objective criterion, provided that the initial population of process design had enough individuals without convergence problems. It can handle multi objective constrained optimization problems involving mixed variables (boolean, integer, real). Constraints as well as Pareto domination principles can be handled by these algorithms. Notice that we add pauses for every ten generations with programming. During each pause all the variables of the previous generation could be stored and outputted to Excel, then the genetic algorithm could restart from the paused generation.

We selected the Non Sorted Genetic Algorithm II (NSGAI) for process optimization. NSGAI is based on a ranking procedure, where the rank of each solution is defined as the rank of the Pareto front which it belongs to. The diversity of non dominated solutions is guaranteed by using a crowding distance measurement, which is an estimation of the size of the largest cuboids enclosing a given solution without including any other.

2.3. Objective functions

In this study, four objective functions are used in MOGA method for the optimization of the extractive distillation. The first objective function is energy cost per unit product OF with some modifications [24]. It is also the sole objective function used in the TSOM method under given tray numbers of the columns (N_1 and N_2) and specified $x_{H,I,E}$.

$$\begin{aligned} \min OF &= \frac{M \cdot Q_{r1} + m \cdot Q_{c1} + M \cdot Q_{r2} + m \cdot Q_{c2}}{D_2} \\ \text{subject to: } &x_{\text{water}, D_1} \geq 0.999 \\ &x_{\text{water}, W_1} \leq 0.0001 \\ &x_{AA, D_2} \geq 0.999 \\ &x_{NMA, W_2} \geq (1 - x_{H,I,E}) \text{ or variable} \end{aligned} \quad (1)$$

Since D_1 product is water and it will be recycled to the origin production process, no need treating it at denominator. Constraint 1 concerns the product (water) purity. It is necessary for reducing the entrainer NMA losses and AA purity following the interrelationship among distillates [29]. Constraint 2 in bottom W_1 (F_2) aims at keeping high the product (water) recovery. Constraint 2 is also imperative because water will be the main impurity in D_2 , too much water entering regeneration column will prevent the achievement of high purity AA at D_2 . Constraint 3 serves the product (AA) purity in D_2 . Constraint 4 focuses on the recycling entrainer purity, which could be specified in TSOM method and optimized through sensitivity analysis, and could be regarded as variable in MOGA method. The meanings of the notations Q_{r1} , Q_{c1} , Q_{r2} , Q_{c2} , D_1 and D_2 , are shown in Fig. 3. The energy price difference factor m equals to 0.036 for condenser (cooling water) vs reboiler (low pressure steam). M may equal to 1, 1.065 or 1.280 when low, middle or high pressure steams are used, respectively. The process utilities are shown in Table C1 in Appendix B. Therefore, the meaning of OF is the energy consumption used per product unit flow rate (kJ/kmol). It accounts for both columns and also reflects the weight coefficient of the reboiler – condenser heat duty.

TAC has been commonly used directly as an optimization criterion [28]. Here as the second objective function, it is calculated to compare the different designs. TAC includes capital cost per year and operating costs as shown the following formula:

$$TAC = \frac{\text{capital cost}}{\text{payback period}} + \text{operating costs} \quad (2)$$

For computing the capital cost, Douglas’ cost formulas [28] are employed after transferred into CEPCI inflation index. The column shell, tray and heat exchanger cost constitute the capital cost and their formulas are shown in Appendix A. The CEPCI in 2013 (567.3) [29] and

a three year payback period are used for calculating the capital cost. The operating cost contains the energy cost in reboiler and condenser. The heat exchanger for cooling the recycling entrainer is taken into account in order to emphasize its effect on the process. Other costs such as the liquid delivery pumps, pipes, valves are neglected at the conceptual design stage that we consider.

The third and four objective functions are the efficiency indicators of extractive section E_{ext} and the efficiency indicator per tray in extractive section e_{ext} as both have been defined in previous works [25]. They have the ability to discriminate the desired product between the top and the bottom of the extractive section, which is the key part of the extractive distillation. E_{ext} is defined as follow

$$E_{ext} = x_{p,H} - x_{p,L} \quad (3)$$

Where $x_{p,H}$ is the product mole fraction at the entrainer feed tray, which is also the location of the stable node of the extractive section. And $x_{p,L}$ is the product mole fraction at fresh feed tray.

The definition of e_{ext} is as follow

$$e_{ext} = \frac{E_{ext}}{N_{ext}} \quad (4)$$

Where N_{ext} is the tray number in the extractive section. And e_{ext} is a beneficial complement to E_{ext} for handling the different designs with different entrainer to feed flow rate ratio, different reflux ratio and different tray number in the extractive section.

3. Results and discussions

3.1. Thermodynamic analysis of AA dehydration with NMA

For water-AA with NMA system, the ternary RCM belongs to class 0.0 1 and not exhibiting any univolatility line. If the general $x_{L,I,E}$ strategy is implemented, high purity NMA should be defined at the bottom liquid of the regeneration column. Unfortunately, there is a tangent VLE point between AA and NMA at NMA rich region (see Fig. 1), which will cause the dramatically increase of reflux ratio and the reboiler duty for achieving a NMA high purity. This will counteract the energy saving potential of the extractive distillation compared with conventional distillation process, which goes against to our intention.

Following the thermodynamic analysis in Section 2, when a high purity recycling entrainer NMA (strategy $x_{L,I,E}$) reenters into the extractive column, the point $SN_{ext,A}$ arises and it is located very close to the on the binary edge water-NMA of the ternary map (see Fig. 2d) and intersect a residue curve for reaching the vertex A (water). While recycling entrainer stream with a lower purity (strategy $x_{H,I,E}$) which reenters into the extractive column, this option provides the intersection point between the rectifying and extractive liquid profile in a point which is a little bit higher than the $SN_{ext,A}$, and then intersects another residue curve for reaching the vertex A (water). Of course, the penalty of increasing the trays in rectifying section and the reflux ratio in the extractive column is unavoidable since the entrainer with high content of impurities is recycled back. But the process is still suitable to achieve high purity product A (water). This phenomenon for class 0.0 1 is totally different from that of class 1.0 1a, in which low purity recycled entrainer will prevent the high purity of distillate product A. Following the general feasibility rule published by Rodriguez Donis et al. [22] the reason is that the distillate product is an extractive stable node in class 0.0 1 instead of an extractive saddle node in class 1.0 1a, in which the rectifying section profile will apart from and turn off at the saddle node following the residue curve towards the minimum boiling binary azeotrope. This phenomenon prevents achieving of high purity distillate product. In summary, the proposed strategy $x_{H,I,E}$ is feasible for separating mixtures of class 0.0 1 from theoretical analysis and the withdrawal of distillate product with the high required purity is feasible with a reasonable energy consumption and TAC.

3.2. Optimization results of TSOM

In this section, we aim at showing the optimization of TSOM method in retrofitting the extractive distillation process and supplying a comparison for the MOGA results. We use the design in ‘‘Case Ref’’ as initial design [30] where the strategy of high purity recycled entrainer was employed ($x_{L,I,E} = 1 \times 10^{-4}$) and kept the same total tray numbers of the extractive column ($N_1 = 30$) and of the entrainer regeneration column ($N_2 = 20$). The equimolar feed with a flow rate of 500 kmol/h and the entrainer feed are both preheated to 320 K. We set up the same product purity specifications (0.999 molar fraction) for both water and AA and used the same thermodynamic model as ‘‘Case Ref’’. We specify $x_{H,I,E}$ as 0.01 in this part by following the proposed strategy with the sake of alleviating the tangential behavior of VLE between NMA and AA as explained in Section 3.1. The optimal value of $x_{H,I,E}$ is achieved in Section 3.4 by using MOGA method in close loop flowsheet. In this section preliminary design parameters are obtained from simulation and optimization within the open loop flowsheet and further rechecked in the close loop flowsheet.

3.2.1. Choice of D_1 and D_2 with TSOM optimization of F_E , R_1 , R_2

Since the effects of D_1 and D_2 on the product purities are strongly non linear and revealed by their interrelationships [26], D_1 and D_2 were varied with a discrete step of 0.1 kmol/h from 250 kmol/h to 250.2 kmol/h. The SQP optimization was run for F_E , R_1 and R_2 with the initial optimal design: $N_1 = 30, N_2 = 20, N_{FE} = 3, N_{FAB} = 8, N_{FReg} = 7$. No notice that the tray number is counted from top to bottom of the column, and condenser and reboiler are considered as the first and last tray. The results are shown in Fig. 4.

From Fig. 5, we observe that (1) effect of D_1 on OF exists even if there is not D_1 in the denominator part of OF [Eq. (1)]. Previous works have proved that OF could be used satisfactorily for optimizing the two columns together [25,26]. Furthermore, the better OF value is found at $D_1 = 250.1$ kmol/h, instead of the lower value of 250 kmol/h or the higher value 250.2 kmol/h at given D_2 . (2) It seems that OF will decrease by following the increasing direction of D_2 since D_2 is the sole denominator in OF expression. However, OF decreases with decreasing D_2 (see Fig. 5) at constant D_1 . It suggest that there is an optimal value for D_1 as well as the difficulty of separating the binary mixture AA and NMA because of the tangential behavior of VLE at high NMA composition. As we will optimize other variables such as N_{FE} , N_{FAB} and N_{FReg} in the subsequent steps, we select the pair of $D_1 = 250.1$ kmol/h and $D_2 = 250$ kmol/h, corresponding to a product recovery high enough but not too high so as to make the flow sheet convergence difficult. The related OF value is 246521.2 kJ/kmol, with $F_E = 182.4$ kmol/h, $R_1 = 2.107$ and $R_2 = 1.3$.

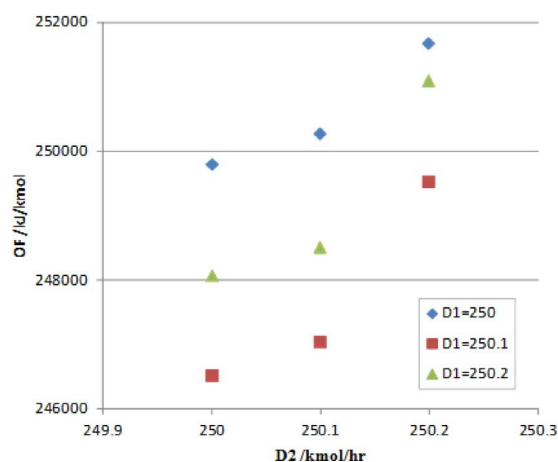


Fig. 5. Effects of D_1 and D_2 on OF with D_1 , D_2 , F_E , R_1 and R_2 as variables.

Table 1

Open loop optimal results of F_E , R_1 , R_2 , N_{FE} , N_{FAB} , N_{FReg} under fixed D_1 and D_2 for the extractive distillation of water – AA with NMA.

No.	N_{FE}	N_{FAB}	N_{FReg}	F_E	R_1	R_2	OF kJ/kmol
1	3	8	7	187.5	2.02	1.38	244603.1
2	3	9	6	160.0	1.89	1.31	233614.1
3	3	12	6	112.6	1.41	0.88	193127.6
4	3	13	6	115.9	1.20	0.91	184532.1
5	4	11	7	106.9	1.52	1.00	200081.1
6	4	12	5	108.7	1.37	0.93	192637.7
7	4	13	6	166.4	0.90	1.05	182292.3
8	4	13	7	165.3	0.91	1.15	185520.7
9	4	14	6	192.5	0.82	1.21	187180.6
10	5	12	5	183.7	0.78	1.13	182512.4

3.2.2. Optimization of the three feed locations

The sensitivity analysis over the three feed locations with ranges [2; 25] for N_{FE} , [$> N_{FE}$; 29] for N_{FAB} and [3; 15] for N_{FReg} were made by using experimental planning procedure [25] so as to avoid the local minimum. For each set of values of N_{FE} , N_{FAB} and N_{FReg} , the variables F_E , R_1 , R_2 are optimized while D_1 and D_2 are fixed. Table 1 shows the results where the design No.1 represents the optimal design for “Case Ref”.

From Table 1, we can conclude that (1) the suitable feed locations allow decreasing the energy cost per unit product OF, as seen by comparing design No. 1 with all other designs. The three feed locations and three continuous variables affect each other and it demonstrates the necessary for optimizing the three feed locations together. (2) The feed location of entrainer moves one tray down the column from design No.1 to No.7 with the lowest OF value. It agrees with the proverbial fact that increasing the tray number in the rectifying section allows decreasing the reflux ratio R_1 . (3) The minimum value of OF is found in design No. 7 with four extra trays in the extractive section than design No. 1. The four more trays have a positive effect on the process and increase the efficiency of the extractive section pushing the location of the extractive stable node $SN_{ext,A}$ near to the edge water NMA as demonstrated in Section 3.2.3. (4) A lower F_E and a higher R_1 in designs No. 3-6 than that in design No. 7 provide a higher OF. Meanwhile a higher F_E and a lower R_1 in designs No. 9 and 10 than that in design No.7 lead also a higher OF. This proves quantitatively that there is a balance between the entrainer usage and the energy cost. (5) Comparing designs No. 7 and 8, we find that only one tray more for N_{FReg} changes the optimal values of the three continuous variables and affects the energy cost OF. It indicates that OF can account the two columns’ variables together. (6) The lowest energy cost for per unit product OF is 182292.3 kJ/kmol. It represents a 25% decrease compared to design No.1 of “Case Ref”.

3.2.3. Effect of high content of impurities in the recycled entrainer on the process

In order to avoid the convergence problems, all the optimization procedure done above was run in the open loop flow sheet (Fig. 4b) with $x_{H,I,E}$ as 0.01 based on the topological thermodynamic analysis of class 0.0-1 in Section 3.1. Therefore, a simulation was re-ran in the closed loop flowsheet (Fig. 3a) for the optimized results $N_{FE} = 4$, $N_{FAB} = 13$, $N_{FReg} = 6$, $F_E = 166.4$ kmol/h, $R_1 = 0.90$ and $R_2 = 1.05$ for which OF = 182292.3 kJ/kmol. The Wegstein tear method was employed to ensure convergence. Design No. 7 satisfied the product purity specification under $x_{H,I,E}$ as 0.01 in the close loop flowsheet. The simulation results are shown in Table 2 as case TSOM. The sizing parameters for the columns and cost data of the design “Case Ref” and case TSOM are shown in Table D1 in Appendix B.

Remarkably, Table 2 shows that the proposed new strategy of high content of impurities in recycled entrainer could successfully improve the extractive distillation process for water-AA-NMA system while keeping the same tray number in the extractive and regeneration

Table 2

Optimal design parameters and cost data from closed loop simulation for the extractive distillation of water – AA with NMA.

column	Case Ref		Case TSOM	
	C ₁	C ₂	C ₁	C ₂
N_1	30		30	
F_{AB} /kmol/h	500.0		500.0	
W_2 /kmol/h	427.3		166.3	
$E_{make\ up}$ /kmol/h	7.44		0.11	
F_E /kmol/h	427.3		166.4	
$x_{H,I,E}/10^{-4}$	1		100	
D_1 /kmol/h	250		250.1	
N_{FE}	3		4	
N_{FAB}	8		13	
R_1	3.00		0.90	
Q_C /MW	11.35		5.39	
Q_R /MW	15.12		7.19	
N_2		20		20
D_2 /kmol/h		250.0		250.0
N_{FReg}		7		6
R_2		2.00		1.05
Q_C /MW		6.79		3.46
Q_R /MW		6.92		3.66
AA purity	0.990		0.999	
$E_{ext}/10^3$	71.2		195	
$e_{ext}/10^3$	11.9		19.5	
TAC/ 10^6 \$/y	6.753		3.235	
OF/kJ/kmol	368820.1		182292.3	

columns. The proposed strategy $x_{H,I,E}$ enables to save energy cost by both alleviating the tangential pinch point of the VLE between AA and NMA and reducing the entrainer flow rate when comparing “Case Ref” and case TSOM.

From Table 2, we also know that (1) The entrainer flow rate decreased drastically from 427.3 kmol/h in “Case Ref” to 166.3 kmol/h in case TSOM as there is no minimum entrainer to feed flow rate ratio explained in Section 2.1. It demonstrates that too much entrainer provides a worse design instead of a better one since the reboiler duty of the regeneration column in “Case Ref” is 1.9 times than that in case TSOM. Besides, the reboiler temperature in “Case Ref” is high due to the low content of impurities in the recycled entrainer, so that high pressure steam is needed. On the contrary, the reboiler temperature in case TSOM is relatively low due to the high content of impurities in the recycled entrainer, and middle pressure steam is enough for heating. (2) Energy consumption showing through OF value in case TSOM is reduced by 20.2% and 50.6% compared with “Case Ref”, respectively. (3) From economical view, TAC in case TSOM is reduced by 52.1% compared with “Case Ref”. It is mainly due to the decreasing of entrainer flow rate, the reflux ratio, the column diameters and the heat exchanger areas in the two columns.

(4) A counter intuitive phenomenon is observed that the efficiency indicators E_{ext} and e_{ext} describing the ability of the extractive section to discriminate the distillate product between the top and the bottom of that section are increased from 0.0712 and 0.0119 in “Case Ref” to 0.195 and 0.0195 in case TSOM, although both high reflux ratio R_1 and entrainer flow rate F_E are used in “Case Ref”. Following the definition of efficiency indicator [25] the increasing of the reflux ratio is useful for E_{ext} whereas the increasing of the entrainer flow rate has adverse effect on the E_{ext} when the F_E gets far enough from than its minimum value. Thus, the reason for the counter intuitive phenomenon is that too much entrainer is used in “Case Ref” having a negative effect over the energy consumption and TAC. On the other hand, both efficiency indicators demonstrate that the extractive section for the case TSOM is more effective than that in “Case Ref” (6) Four more trays are used in the extractive section in case TSOM. This point proves the statement that there should be enough trays in the extractive section in order to achieve the stable node of the extractive section SN_{ext} closer to the edge

water NMA as it is shown in Section 2.1.

In conclusion, Table 2 demonstrates the importance of optimizing the two columns together since the entrainer flow rate in the extractive column is the dominant factor for the regeneration column, and the purity of recycled entrainer has a strong effect on the product purity and energy cost in the extractive column.

3.3. Optimization results of MOGA

3.3.1. Process statement

In order to find the optimal value of $x_{H,I,E}$ in the high content of impurities in the recycled entrainer stream and the optimal total number of trays in the two columns (N_1, N_2), the multi objective genetic algorithm tool available in MATLAB with coupled with Aspen plus process simulator is adopted as optimization variables. The indicator E_{ext} and e_{ext} are also used as objective functions along with the energy cost per unit product OF and TAC. Notice that OF and TAC are minimized while E_{ext} and e_{ext} are maximized.

The tuning process was done for selecting the parameters of genetic algorithm. Several tests were conducted with different values of initial population, crossover and mutation fractions. After tuning, a large number of 300 individuals per generation is chosen. Other parameters were 0.9 for crossover fraction, and 0.1 for mutation fraction. The stop criterion of the genetic algorithm is that the TAC can't be reduced for 30 successive generations. The number of generations achieved 340 in this study.

The eleven optimization variables of the extractive distillation processes are $N_1, N_2, N_{FE}, N_{FAB}, N_{FReg}, D_1, D_2, R_1, R_2, F_E$ and $x_{H,I,E}$. The value ranges are [15,80] for N_1 and N_2 , [15,80] for N_{FE}, N_{FAB} and N_{FReg} (some invalid situations such as $N_{FE} > N_{FAB}, N_{FAB} > N_1, N_{FReg} > N_1$ are excluded by Matlab programming), [248.0, 255.0] for D_1 and D_2 , [0.1, 8] for R_1 and R_2 , [0,0.5] for $x_{H,I,E}$. Notice that the operating pressures of extractive column and entrainer generation column are set at 1 atm. The pressure drop per tray and the tray efficiency are the same as that in TSOM method.

3.3.2. Pareto front of the optimal design solution

The Pareto front of the four objectives are obtained as the result of the MOGA. We choose the design with the minimum TAC as the optimal one from economical practice while the other objective functions are used for analyzing the main insights of the extractive distillation. Generally, the energy cost OF decreases with the increasing of the total tray number in columns, but it is useful for finding the minimum energy cost of each design. Regarding e_{ext} , it is used to avoid the situation that only maximizing E_{ext} will result in too many trays used in extractive section and providing the separation with high TAC. Fig. 6 shows the Pareto front of TAC versus E_{ext} and R_1 , and Fig. 7 shows the Pareto front of TAC versus R_1 and F_E . The lowest TAC design called P1 is shown in red color in Figs. 6 and 7. Notice that the product purity and recovery specification are satisfied for all the 300 designs in the Pareto front.

From Fig. 6, we know that (1) following the decreasing of R_1 , both TAC and E_{ext} decrease quickly. The optimal TAC as 2.948×10^6 \$/y requires R_1 as 0.965 and gives E_{ext} value of 0.223 and. (2) For achieving a given E_{ext} , lowering R_1 is a better choice following minimization of TAC by adjusting other variables. In other words, there is a minimum R_1 for a given E_{ext} . (3) For a given R_1 , there is a maximum E_{ext} . Further, the maximum E_{ext} decreases as the R_1 decrease, and the entire maximum E_{ext} composite an elliptical border.

From Fig. 7, we obtain that (1) few designs belonging to the Pareto front in the region of reflux ratio R_1 lower than 2 and entrainer flow rate F_E higher than 150 kmol/h. The reason is that the separating cost in regeneration column increases quickly at a relatively high F_E , resulting in a higher TAC which prevents the designs in this region to be ranked in the Pareto front. (2) The economical suitable range for the entrainer flow rate F_E is between 100 and 150 kmol/h, corresponding to a ratio (F_E/F) of 0.2–0.3, although there is no minimum value of F_E for water

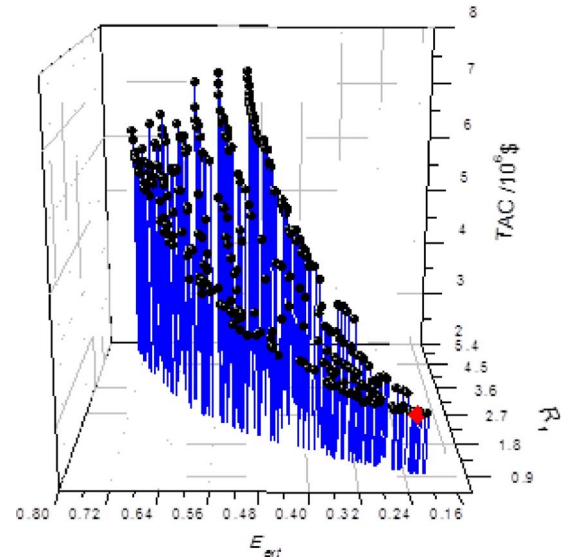


Fig. 6. Pareto front of extractive distillation design for water-AA-NMA system, TAC versus E_{ext} and R_1 , diamond means the lowest TAC.

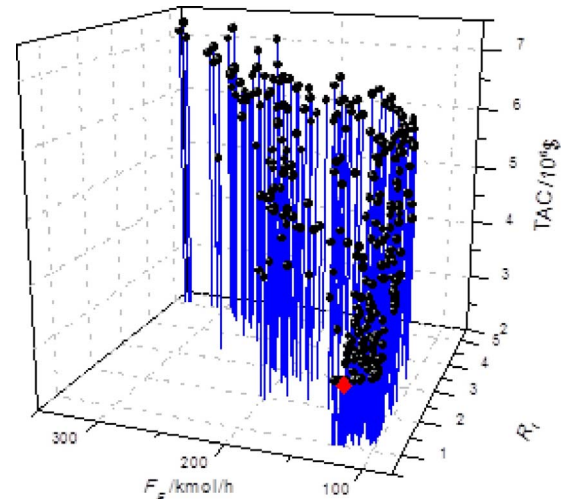


Fig. 7. Pareto front of extractive distillation design for water-AA-NMA system, TAC versus F_E and R_1 , diamond means the lowest TAC.

AA NMA system as explained above from the topological features of class 0.0 1.

3.3.3. Analysis of some designs belonging to Pareto front

The map of E_{ext} vs TAC for the designs belonging to the Pareto front is shown in Fig. 7. There are 287 designs better than "Case Ref" and 40 designs better than case TSOM according to the TAC value. We extract some designs namely P1–P6 for further analysis (see Fig. 8). P1 and P2 are the design with the lowest TAC and the lowest E_{ext} , respectively. P3, P4 and P5 are the designs having similar E_{ext} but different TAC, noticing that P4's TAC is close to that of case TSOM. P6 has a TAC close to that of "Case Ref" but exhibiting much higher E_{ext} . Table 3 shows the design variables of P1–P6 and Table E1 in Appendix B provides the sizing parameters and cost data. Figs. 9 and 10 show the temperature and composition profiles of the extractive column and the regeneration column for the case P1.

Firstly, from Fig. 8 and Table 3 we observe that the P1 design is the optimal design from the MOGA optimization since it exhibits the lowest TAC and OF while the optimal $E_{ext,opt}$ is 0.223 considering equimolar feed composition. Although the tray numbers of columns ($N_1 = 41$ and $N_2 = 28$) are increased, the TAC and energy cost OF for P1 design are

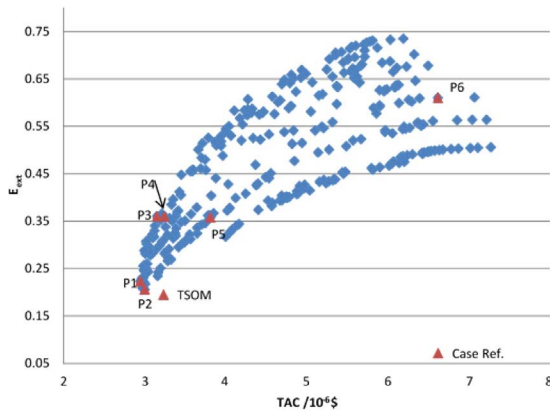


Fig. 8. Map of E_{ext} vs TAC of the designs belonging to the Pareto front.

reduced further by 8.9% and 12.7% compared with the design case TSOM at given $N_1 = 30$ and $N_2 = 20$. It's mainly because of a 26.7% decreasing of entrainer flow rate F_E , and the significant reduction of the reflux ratio R_2 in the regeneration column. It proves that a suitable increasing of the total tray numbers of the columns could reduce the total cost of the process. Remarkably, the is 0.3% for P1 design, which is obtained after optimization unlike that is specified as 1% in the TSOM method. P2 design has the lowest E_{ext} among all the designs belonging to Pareto front where E_{ext} is maximized. However, its E_{ext} (0.210) is still higher than that of case TSOM (0.195) and “Case Ref” (0.0712).

Secondly, the TAC of P4 design is similar to that of case TSOM, but with a much higher efficiency indicator E_{ext} (0.360 of P4 design vs 0.195 of case TSOM). It is mainly because of the lower F_E and the higher R_1 comparing to case TSOM design. Reducing F_E provides a higher water content $x_{p,H}$ at the stable node $SN_{ext,A}$ of the extractive profile and $SN_{ext,A}$ is located on the binary edge water – NMA closer to the water apex (see Fig. 3). Furthermore, the increasing of R_1 drags the unstable separatrix much closer to AA – NMA side and then resulting in a lower water content $x_{p,L}$ at the other end of the extractive profile (the tray above of the fresh feed tray). Therefore, E_{ext} increases following its definition by the equation [3]. A higher water content in $x_{p,H}$ means an

easier water separation in the rectifying section whereas a lower water content $x_{p,L}$ improves the separation of the binary mixture AA – NMA in the stripping section of the extractive distillation column. In other words, the benefit of a higher E_{ext} in P4 design than that in TSOM design is just counteracted by its penalty (high reflux ratio, high column diameter and high heat exchanger area in the extractive column). The results demonstrate that the variables related to E_{ext} , such as R_1 , F_E , N_{FE} , N_{FAB} in both designs P4 and TSOM could be further optimized by a more suitable compromise among the two designs, just as it is shown in Fig. 8 and Table 3 for P1 design providing a better compromise between a lower TAC and a suitable E_{ext} . Therefore, we can infer that a design with an efficiency indicator getting far from a suitable limit for $E_{ext,opt}$ is not well designed such as “Case Ref”, case TSOM and P4 design. It should be noted from Table 3 that P design provides the second better value of E_{ext} , with the lowest TAC and OF hence it can be defined as the reference value of $E_{ext,opt}$.

Thirdly, for the designs of P3, P4 and P5 with nearly the same efficiency indicator E_{ext} , TAC in P3 design is lower 97.4% and 83.8% than those in P4 and P5 design. It's mainly because the smaller entrainer flow rate F_E and reflux ratio R_1 for P3 that induce the decreasing of reboiler and condenser duties, and the logical reducing of OF and TAC. This point proves the importance of reasonable increasing of the tray's number in the extractive section as 15 trays for the design of P3, 11 trays for the design of P4 and 7 trays for the design of P5 providing the same separation involving a lower reflux ratio. This point is in agreement with Lelkes's study [31], the extractive section should have enough trays so that the composition at the entrainer feed tray lies near the stable node of the extractive section $SN_{ext,A}$ that should be close to the product vertex A. Besides, a high extractive efficiency indicator per tray e_{ext} doesn't mean low OF and TAC if the enhance of e_{ext} indicator is caused by decreasing of the tray's number in the extractive section and the consequent increasing of F_E and R_1 in order to get the same E_{ext} . This point is verified by comparing the optimal designs of P3, P4 and P5 in Table 3.

Lastly, P6 design has similar TAC with the design of “Case Ref”, but much higher efficiency indicator E_{ext} . Both designs remind again that a higher or lower E_{ext} from the $E_{ext,opt}$ implies an unreasonable design. P6 design includes an extractive column having the smaller tray's number and then needing the highest entrainer flow rate and reflux ratio. Worst results were obtained for the recovery solvent column with the highest

Table 3
Design parameters for P1-P6 belonging to the Pareto front of water-AA with NMA.

	P1	P2	P3	P4	P5	P6
Extractive column						
N_1	41	39	44	39	36	27
F_{AB} , kmol/h	500.0	500.0	500.0	500.0	500.0	500.0
W_2 , kmol/h	121.9	128.0	75.9	107.2	127.4	249.1
E_{makeup} , kmol/h	0.1	0.1	0.2	0.2	0.2	0.2
F_E /kmol/h	122.0	128.1	76.1	107.4	127.6	249.3
$x_{H,L,E}/10^{-4}$	30	60	10	70	60	40
N_{FE}	5	7	4	5	9	8
N_{FAB}	15	15	18	15	15	15
D_1 /kmol/h	250.1	250.1	250.2	250.2	250.2	250.2
R_1	0.965	0.968	1.364	1.433	2.077	4.996
Q_C /MW	5.575	5.583	6.709	6.905	8.733	17.017
Q_R /MW	7.117	7.160	7.973	8.347	10.297	19.404
Regeneration column						
N_2	28	32	28	22	29	35
D_2 /kmol/h	250.0	250.0	250.0	250.0	250.0	250.0
N_{FReg}	5	6	4	4	5	5
R_2	0.383	0.403	0.334	0.385	0.402	1.495
Q_C /MW	2.337	2.372	2.283	2.372	2.401	4.542
Q_R /MW	2.487	2.539	2.373	2.506	2.573	4.274
OF/kJ/kmol	159045.4	160685.9	170623.0	178969.0	211046.1	392232.0
TAC/ 10^6 \$/y	2.948	2.980	3.169	3.252	3.780	6.626
$E_{ext}/10^3$	223	210	359	360	362	610
$e_{ext}/10^3$	20.3	23.3	23.9	32.7	51.7	76.3

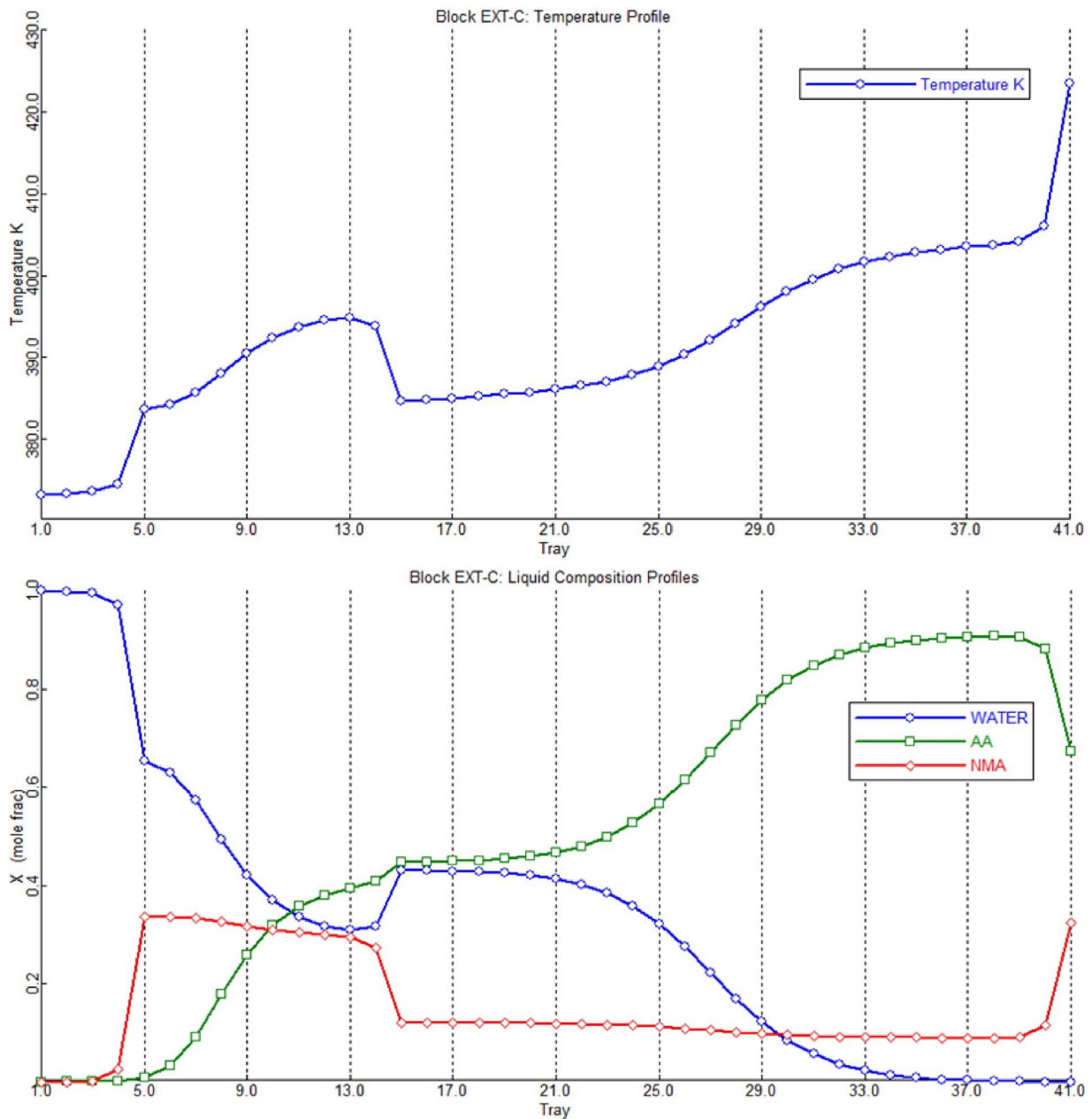


Fig. 9. Temperature and composition profiles of case P1 extractive column for the extractive distillation of water – AA with NMA.

tray's number and reflux ratio compared to other designs.

Regarding the temperature and composition profile of the extractive column and regeneration column of case P1 in Figs. 9 and 10, the fresh mixture feed temperature is relatively low, indicating that it is feasible to preheat the fresh feed temperature for reducing the reboiler duty of extractive column Q_{R1} . In other words, the heat integration between the recycling entrainer stream (hot side) and the fresh feed stream (cold side) is feasible. There is an increasing jump of AA content in the fresh feed tray due to an equimolar feed composition. It suggests that the P1 design can deal with more dilute AA aqueous solution. Importantly, the targeting product water content from N_{FE} tray to N_{FAB} tray increases quickly and it demonstrates that the low F_E and low R_1 in P1 design could be able to achieve enough separation effect in the extractive section, which is quantitatively verified by the efficiency indicators E_{ext} and e_{ext} . Besides, most of the trays (26 trays from total 41) are used in the stripping section for preventing water to exit in the bottom product of the extractive column as the water content decrease slowly and smoothly in the stripping section. Only five trays are used in rectifying

section of regeneration column for achieving a high purity product AA whereas 23 trays are used in the stripping section for approaching a relatively low purity of recycled entrainer. This phenomenon reveals the low relative volatility between AA and NMA at NMA rich side (see Fig. 1).

3.4. Comparisons from ternary map and relative volatility

Fig. 11 shows the ternary liquid composition profiles for designs "Case Ref", TSOM and P1 of the extractive column of water – AA with NMA.

Following remarks can be stated from Fig. 11: (1) the stable node of extractive section SN_{ext} connecting the extractive liquid profile with the rectifying profile for "Case Ref" is very close to the water – NMA side, demonstrating that low content of impurities in the recycled entrainer is achieved ($x_{H,I,E} = 1 \times 10^{-4}$). On the contrary, the impurity content in the recycled entrainer and hence, the SN_{ext} location for the cases TSOM ($x_{H,I,E} = 10 \times 10^{-4}$) and P1 ($x_{H,I,E} = 30 \times 10^{-4}$) are much

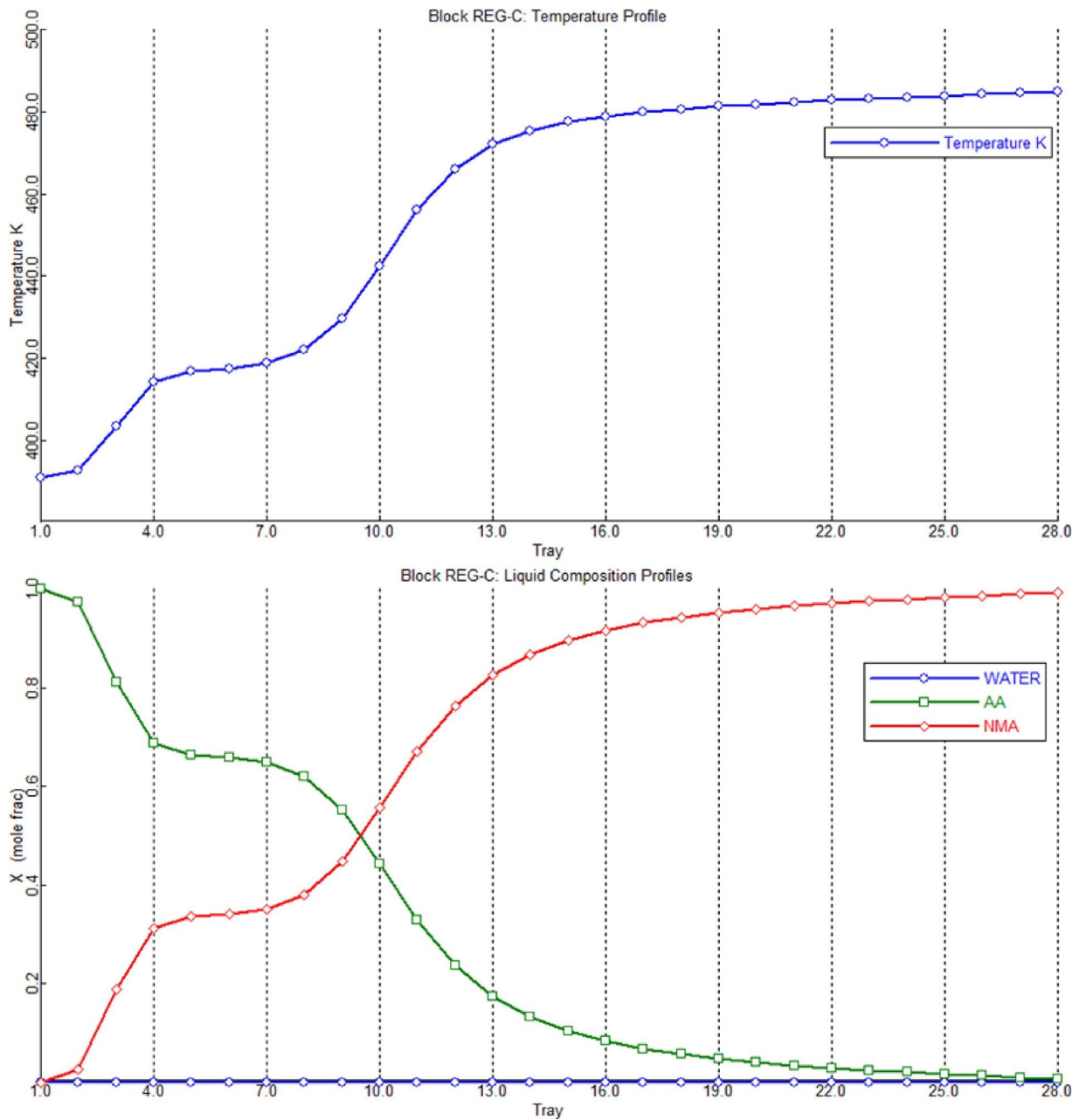


Fig. 10. Temperature and composition profiles of case P1 regeneration column for the extractive distillation of water – AA with NMA.

higher than those of “Case Ref”, corresponding to the proposed new strategy from the thermodynamic analysis discussed in Section 3.1. (2) The separation between water and NMA in the rectifying section is easy since there are only few trays in this section for achieving high purity water at a relatively low reflux ratio. (3) The effect of extractive section (liquid profile limited by F_E and SN_{ext} position) in “Case Ref” is so weak even at high F_E and high R_1 compared with the other two cases. It indicates the importance of finding suitable feed locations N_{FE} and N_{FAB} in addition to the main variables F_E and R_1 . (4) F_E is not the dominant factor for the location of SN_{ext} when the appropriated number of trays is not well established in each section. Indeed, the SN_{ext} position are closer for “Case Ref” and TSOM case even with a relatively large difference of F_E . (5) Most of the trays in the extractive column are used in the stripping section. It demonstrates that the separation of water and AA at AA rich end is difficult even in the presence of the entrainer. It should be noted that the composition of AA in the stripping section reaches 0.9 close to the bottom column. (6) Optimal design is not

straightly related to the location of the extractive liquid profile in the region exhibiting the higher isovolatility values between water and AA. This condition could be simply forced by increasing the entrainer flow rate. The optimal design is determined by the position of the extractive liquid profile with the highest values of relative volatility between water and AA by using the lowest amount of the entrainer. That is the case of design P1 where the extractive liquid profile is located in a similar region of isovolatility values to case TSOM but by using 73.5% of the entrainer only. It should be noted that an entrainer providing high isovolatility lines close to A component apex will enable the separation with lower entrainer flow rate.

It can be observed in Fig. 11 that the rectifying section is used for separating water and NMA instead of water and AA, so it doesn't matter how low is the relative volatility between water and AA $\alpha_{water AA}$. Interestingly, the $\alpha_{water AA}$ in the extractive section decreases quickly while the content of entrainer remains below 0.5 (see Fig. 9) because the average value of $\alpha_{water AA}$ in the extractive section is high in the

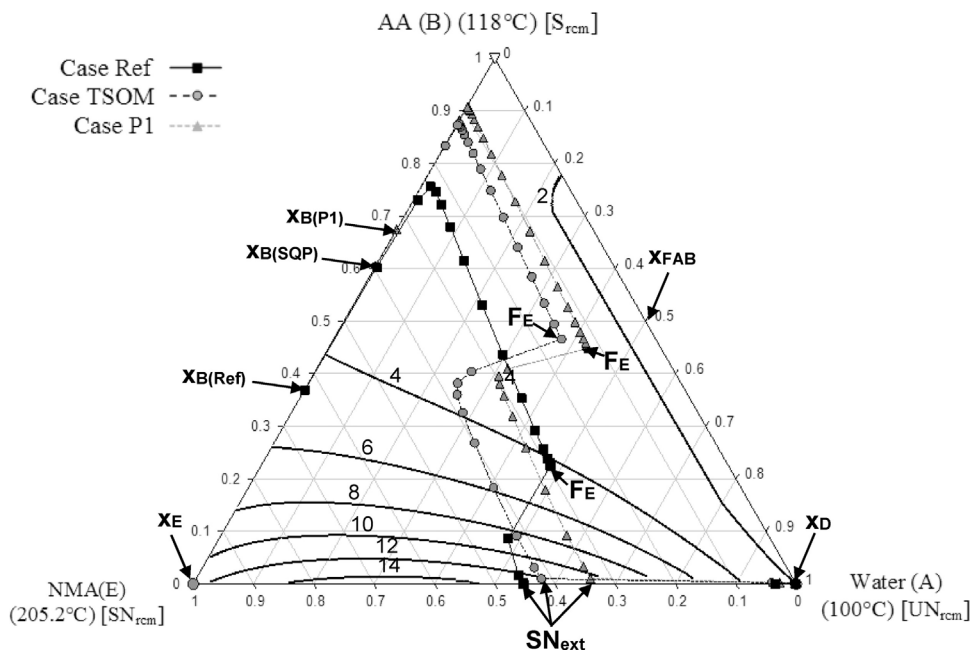


Fig. 11. Ternary liquid composition profiles for “Case Ref”, TSOM and P1 in the extractive column along with the isovolatility curves $\alpha_{\text{water AA}}$.

three cases (between 2 and 12). In the stripping section, the $\alpha_{\text{water AA}}$ is much lower than that in the extractive section (between 2 and 3). This phenomenon is different from other extractive distillation systems such as ethanol water [33], acetone methanol [25], isopropyl alcohol water [32] and so on. The reason is that even there is not azeotrope formation between water and AA, the average relative volatility of water is close to unity (see Fig. 1). This special behavior contributes to the most trays used in the stripping section. Importantly, due to the existence of entrainer NMA, $\alpha_{\text{water AA}}$ becomes higher enough to provide an economical process.

3.5. General remarks

Based on the optimal design results from two optimization methods, some conclusive remarks can be highlighted:

- (1) A new strategy of high content of impurities in the recycled entrainer is set up based on the thermodynamic analysis of the ternary RCM. The new strategy is verified by the optimal design results: the content of water in the extractive node S_{Next} in P1 design is higher than that those obtained in the “Case Ref” shown in Fig. 11. Therefore, S_{Next} in P1 is closer to the product vertex, which hints at less tray number or lower reflux ratio are needed for reaching the required separation.
- (2) Although the feeding entrainer allows increasing the relative volatility of the zeotropic mixture, reducing the entrainer flow rate is useful for reducing the energy consumption in both columns, resulting in that in case P1 the objective function OF is saved by 12.8% and 56.9% compared with the case TSOM and the “Case Ref”, respectively. The optimal entrainer flow rate corresponds to the minimal value needed for placing the liquid profile inside the extractive section in a high relative volatility region. A higher amount of entrainer mainly increases the cost of the extractive distillation process.
- (3) Although N_1 and N_2 in P1 design are higher, the TAC of P1 design is reduced by 28.4% and 56.3% compared with case TSOM and “Case Ref”, respectively.
- (4) More trays are used in the extractive section in case P1 design than that in case TSOM and “Case Ref”. This point proves the statement that enough number of trays has to be defined in the extractive section in order to achieve the optimal position of the stable

extractive node S_{Next} on the edge A E as shown in Fig. 3 (Section 2.1). Furthermore, increasing of number of trays in the extractive section allows separating the key components with lower entrainer flow rate and reflux ratio.

- (5) The most extra total trays of the extractive distillation column in case P1 ($N_1 = 41$) than that in case TSOM ($N_1 = 30$) are used in the stripping section in order to prevent water exiting at the bottom product. It is necessary for achieving high purity of AA product since the water in the extractive bottom product will be an impurity of AA distillate of the second column.
- (6) The pairs of case P6 and “Case Ref”, case P4 and case TSOM remind that a higher or lower E_{ext} from the $E_{\text{ext,opt}}$ implies an unreasonable design because additional cost are related to increasing the reflux ratio or the number of trays.
- (7) The effect of extractive section in “Case Ref” is so weak even the higher entrainer flow rate and reflux ratio that are used comparing with case P1. This indicates the importance of finding suitable feed locations N_{FE} and N_{FAB} in addition to the main variables F_E and R_1 .

4. Conclusions

A novel strategy of high content of impurities in the recycled entrainer was proposed for the AA dehydration extractive distillation with *N* methyl acetamide as entrainer through the analysis of thermodynamic insights of the ternary RCM. The superiority of using NMA compared to other standard entrainers like DMF and DMSO was settled from the analysis of the isovolatility lines map of each resulting ternary mixture. The studied case water-AA-NMA belongs to class 0.0-1 with no univolatility line existing with the particularity that water is the unstable extractive node of the RCM and it is always possible to find suitable operating conditions in the extractive distillation column providing the distillate with the required purity. The proposed strategy could reduce the amount of entrainer in the extractive distillation column and save energy cost in the regeneration column by avoiding the approach of the tangency behavior of the VLE between AA and NMA in the region with high NMA content.

We have run two methods for the process optimization studies: two step optimization method (TSOM) using SQP and the multi objective genetic algorithm (MOGA). From process retrofit view, TSOM is used to minimize the total energy consumption per product unit OF at a given tray number of columns and a fixed content of impurities in the

recycled entrainer. Conversely, MOGA is implemented by relaxing the content of impurities in the recycled entrainer and the tray numbers of the two columns through minimizing OF and TAC, and maximizing a thermodynamic separation factor E_{ext} and e_{ext} in the extractive section of the extractive distillation column. Here the high content of impurities in the recycled entrainer is a variable instead of specification. The Pareto front is obtained as the results with a total of eleven variables being optimized.

Thanks to the optimization under the new strategy, significant cost savings are achieved. Energy consumption OF is reduced by 12.8% and 56.9% whereas TAC is saved by 28.4% and 56.3% compared with optimal case TSOM and the “Case Ref”, respectively. Through the analysis of Pareto front, the effects of the main variables on TAC and efficiency indicator were discussed. Two important issues have emerged. First the proposed strategy is beneficial to the AA dehydration extractive distillation. Second, a higher or lower efficiency indicator from the $E_{ext,opt}$

could imply an unreasonable design, and the definition of an acceptable value for $E_{ext,opt}$ could be regarded as a relevant criterion to assess the performance of an optimal extractive distillation process design. We have also noticed that a suitable shift of the feed tray locations improves the efficiency of the separation, mainly when less entrainer is used. The optimal design is given by the location of the extractive liquid profile inside the extractive distillation column in a region of high relative volatility values between the components to be separated and by using the lower entrainer flow rate.

Acknowledgements

This work was supported by the Doctoral Fund of Ministry of Education of China (No. 2016M601528) and the National Natural Science Foundation of China (No. 21606026 and 21276073).

Appendix A

The diameter of a distillation column is calculated using the *tray sizing* tool in Aspen Plus software.

The height of a distillation column is calculated from the equation:

$$H = \frac{N}{e_T} \times 0.6096 N \text{ tray stage except condenser and reboiler, } e_T \text{ tray efficiency is taken as 85\% for calculating TAC.}$$

The heat transfer areas of the condenser and reboiler are calculated using following equations:

$$A = \frac{Q}{u \times \Delta T} \text{ u: overall heat transfer coefficient (kW K}^{-1} \text{ m}^{-2}\text{), u = 0.852 for condenser, 0.568 for reboiler.}$$

The capital costs of a distillation column are estimated by the following equations:

$$\text{Shell cost} = \left(\frac{CEPCI}{100}\right) \times 902.8 \times D^{1.066} H^{0.802} \times (2.18 + F_C) = 22688.6 D^{1.066} H^{0.802} \text{ Unit of D and H: m}$$

$$\text{Tray cost} = \left(\frac{CEPCI}{100}\right) \times 93.1 \times D^{1.55} H F_C = 1426.0 D^{1.55} H \text{ Unit of D and H: m}$$

$$\text{Heat Exchanger cost} = \left(\frac{CEPCI}{100}\right) \times 457.4 \times A^{0.65} \times (2.29 + F_C) = 9367.8 A^{0.65} \text{ Unit of A: m}^2$$

Table A1
Association parameters of HOC equation for AA-water-NMA.

component	water	AA	NMA
water	1.7	2.5	0
AA	2.5	4.5	0
NMA	0	0	0

Appendix B

Table B1
NRTL binary parameter of water-AA-NMA.

Component	water	water	AA
	AA	NMA	NMA
aij	3.3293	0.2677	0
aji	1.9763	0.4428	0
bij	723.888	1024.883	446.521
bji	609.8886	660.244	49.23936
cij	0.3	0.3	0.3

Table C1
Utility.

Name	Pressure/MPa	Temperature/K	Price/\$/GJ
LP steam	0.5	433	7.72
MP steam	1.0	457	8.22
HP steam	1.5	527	9.88
Cooling water	0.1	298	0.278

Table D1
Sizing parameters for the columns and cost data of the design case ref and case TSOM.

	Case ref	Case TSOM
	Extractive column	
Diameter/m	3.214	2.236
Height/m	20.12	20.12
$I_{CS}/10^6\$$	0.875	0.594
A_C/m^2	191	91
A_R/m^2	373	445
$I_{HE}/10^6\$$	0.730	0.674
$Cost_{cap}/10^6\$$	1.780	1.368
$Cost_{ope}/10^6\$$	3.953	1.572
$Cost_{CA}/10^6\$$	4.547	2.028
	Regeneration column	
Diameter/m	2.092	1.477
Height/m	13.42	13.42
$I_{CS}/10^6\$$	0.400	0.276
A_C/m^2	91	47
A_R/m^2	279	146
$I_{HE}/10^6\$$	0.544	0.355
$Cost_{cap}/10^6\$$	1.004	0.666
$Cost_{ope}/10^6\$$	1.822	0.962
$Cost_{CA}/10^6\$$	2.157	1.184
Q_{HA}/MW	3.132	1.214
$Cost_{HA}/10^6\$$	0.049	0.023
OF/kJ/kmol	368820.1	182292.3
TAC	6.753	3.235
$E_{ext}/10^3$	71.2	195
$e_{ext}/10^3$	11.9	19.5

Table E1
Sizing parameters for the columns and cost data of the design P1-P6 belonging to Pareto front, water-AA with NMA.

	P1	P2	P3	P4	P5	P6
	Extractive column					
Diameter/m	2.221	2.229	2.387	2.447	2.737	3.850
Height/m	28.05	26.83	30.48	26.83	24.39	18.29
$I_{CS}/10^6\$$	0.770	0.746	0.889	0.824	0.860	0.983
A_C/m^2	94	94	113	116	147	286
A_R/m^2	396	398	443	464	572	1078
$I_{HE}/10^6\$$	0.641	0.643	0.700	0.719	0.828	1.257
$Cost_{cap}/10^6\$$	1.549	1.522	1.756	1.695	1.853	2.450
$Cost_{ope}/10^6\$$	1.557	1.566	1.747	1.829	2.257	4.257
$Cost_{CA}/10^6\$$	2.073	2.073	2.333	2.394	2.875	5.074
	Regeneration column					
Diameter/m	1.214	1.222	1.188	1.210	1.222	1.650
Height/m	18.90	21.95	18.90	14.64	19.51	23.78
$I_{CS}/10^6\$$	0.295	0.335	0.288	0.240	0.305	0.492
A_C/m^2	32	32	31	32	33	58
A_R/m^2	102	104	97	103	105	186
$I_{HE}/10^6\$$	0.279	0.282	0.272	0.281	0.285	0.412
$Cost_{cap}/10^6\$$	0.610	0.660	0.595	0.548	0.627	0.977
$Cost_{ope}/10^6\$$	0.654	0.668	0.625	0.659	0.677	1.194
$Cost_{CA}/10^6\$$	0.857	0.888	0.823	0.842	0.886	1.520
Q_{HA}/MW	0.902	0.954	0.563	0.786	0.946	1.865
$Cost_{HA}/10^6\$$	0.018	0.019	0.013	0.016	0.019	0.032
OF/kJ/kmol	159045.4	160685.9	170623.0	178969.0	211046.1	392232.0
TAC	2.948	2.980	3.169	3.252	3.780	6.626
$E_{ext}/10^3$	223	210	359	360	362	610
$e_{ext}/10^3$	20.3	23.3	23.9	32.7	51.7	76.3

References

- [1] W.T. Hess, A.N. Kurtz, D.B. Stanton, Kirk-Othmer Encyclopedia of Chemical Technology, John Wiley & Sons Ltd., New York, 1995.
- [2] B. Saha, S.P. Chopade, S.M. Mahajani, Recovery of dilute acetic acid through esterification in a reactive distillation column, Catal. Today 60 (2000) 147–157.
- [3] V. Van Brunt, Process for recovering acetic acid from aqueous acetic acid solutions. 1992. US Patent No. 5, 175, 357.
- [4] S. Kürüm, Z. Fonyo, Comparative study of recovering acetic acid with energy integrated schemes, Appl. Therm. Eng. 16 (1996) 487–495.
- [5] N.V. Long, S. Lee, M. Lee, Design and optimization of a dividing wall column for debottlenecking of the acetic acid purification process, Chem. Eng. Process. 49 (2010) 825–835.
- [6] S.K. Wasylkiewicz, L.C. Kobylka, F.J.L. Castillo, Optimal design of complex azeotropic distillation columns, Chem. Eng. J. 79 (2000) 219–227.
- [7] I. Chien, K.L. Zeng, H.Y. Chao, J.H. Liu, Design and control of acetic acid dehydration system via heterogeneous azeotropic distillation, Chem. Eng. Sci. 59 (2004) 4547–4567.
- [8] I. Chien, C.L. Kuo, Investigating the need of a pre-concentrator column for acetic

- acid dehydration system via heterogeneous azeotropic distillation, *Chem. Eng. Sci.* 61 (2006) 569–585.
- [9] Z. Lei, C. Li, Y. Li, B. Chen, Separation of acetic acid and water by complex extractive distillation, *Sep. Purif. Technol.* 36 (2004) 131–138.
- [10] W. Muller, Method for the separation of acetic acid by extractive rectification. 1975. US Patent No. 3, 878, 241.
- [11] R. Sartorius, H. Stapf, Process for preparing technically pure acetic acid by extractive distillation. 1976. US Patent No.3, 951, 755.
- [12] L.R. Cohen, Method for separating carboxylic acids from mixtures with non-acides. 1986. US Patent No. 4, 576, 683.
- [13] L. Berg Dehydration of acetic acid by extractive distillation, 1992. US Patent No. 5, 167, 774.
- [14] X.L. Hu, R.Q. Zhou, Influence of nitrogen containing complexing agents on the vapor-liquid equilibrium of water-acetic acid systems, *Fine Chem.* 19 (2002) 612–614.
- [15] V.N. Kiva, E.K. Hilmen, S. Skogestad, Azeotropic phase equilibrium diagrams: a survey, *Chem. Eng. Sci.* 58 (2003) 1903–1953.
- [16] H. Renon, J.M. Prausnitz, Local compositions in thermodynamic excess functions for liquid mixtures, *AIChE J.* 14 (1968) 135–144.
- [17] J.G. Hayden, J.P. O'Connell, A generalized method for predicting second virial coefficients, *Ind. Eng. Chem. Proc. Des. Dev.* 14 (1975) 209–216.
- [18] W. Chang, H. Wan, G. Guan, H. Yao, Isobaric vapor-liquid equilibria for water + acetic acid + (N-methyl pyrrolidone or N-methyl acetamide), *Fluid Phase Equilib.* 242 (2006) 204–209.
- [19] J. Gmehling, U. Onken, Vapor-liquid equilibrium data collection, in: D. Behrens, R. Eckermann (Eds.), *DECHEMA Chemistry Data Series*, DECHEMA Publishers, Frankfurt, Germany, 1977.
- [20] ProSim S.A., <http://www.prosim.net>.
- [21] Y. Peng, L. Ping, S. Lu, J. Mao, Vapor-liquid equilibria for water + acetic acid + (N,N-dimethylformamide or dimethyl sulfoxide) at 13.33 kPa, *Fluid Phase Equilib.* 275 (2009) 27–32.
- [22] I. Rodriguez-Donis, V. Gerbaud, X. Joulia, Thermodynamic insights on the feasibility of homogeneous batch extractive distillation, 2. Low relative volatility binary mixtures with a heavy entrainer, *Ind. Eng. Chem. Res.* 48 (2009) 3560–3572.
- [23] J.P. Knapp, M.F. Doherty, Minimum entrainer flows for extractive distillation: a bifurcation theoretic approach, *AIChE J.* 40 (1994) 243–268.
- [24] X. You, I. Rodriguez-Donis, V. Gerbaud, Extractive distillation process optimisation of the 1.0-1a class system, acetone-methanol with water, in: J.J. Klemes, S.V. Varbanov, P.Y. Liew (Eds.), *24th European Symposium on Computer Aided Process Engineering*, Elsevier, Amsterdam, 2014 ISBN 978-0-444-63456-6.
- [25] X. You, I. Rodriguez-Donis, V. Gerbaud, Improved design and efficiency of the extractive distillation process for acetone-methanol with water, *Ind. Eng. Chem. Res.* 54 (2015) 491–501.
- [26] X. You, I. Rodriguez-Donis, V. Gerbaud, Low pressure design for reducing energy cost of extractive distillation for separating diisopropyl ether and isopropyl alcohol, *Chem. Eng. Res. Des.* 109 (2016) 540–552.
- [27] M. Vázquez-Ojeda, J.G. Segovia-Hernández, S. Hernández, A. Hernández-Aguirre, A.A. Kiss, Design and optimization of an ethanol dehydration process using stochastic methods, *Sep. Purif. Technol.* 105 (2013) 90–97.
- [28] J.M. Douglas, *Conceptual Design of Chemical Processes*, McGraw-Hill, New York, 1988.
- [29] CEPICI, CEPICI index for year 2013, *Chem. Eng.* 123 (2016) 92.
- [30] Z. Denglei, T. Chao, R. Genkuan, Concept design and optimization by aspen plus for extractive distillation, *Comp. Appl. Chem.* 6 (2010) 791–795.
- [31] Z. Lelkes, P. Lang, B. Benadda, P. Moszkowicz, Feasibility of extractive distillation in a batch rectifier, *AIChE J.* 44 (1998) 810–822.
- [32] S. Arifin, I.L. Chien, Design and control of an isopropyl alcohol dehydration process via extractive distillation using dimethyl sulfoxide as an entrainer, *Ind. Eng. Chem. Res.* 47 (2008) 790–803.
- [33] S.H. Luo, C.S. Bildea, A.A. Kiss, Novel heat-pump-assisted extractive distillation for bioethanol purification, *Ind. Eng. Chem. Res.* 54 (2015) 2208–2213.